Physica Medica 112 (2023) 102610

Contents lists available at ScienceDirect

Physica Medica

journal homepage: www.elsevier.com/locate/ejmp

Normative values of the topological metrics of the structural connectome: A multi-site reproducibility study across the Italian Neuroscience network

Pasquale Borrelli [a], Giovanni Savini [b], Carlo Cavaliere [a], Fulvia Palesi [c], Maria Grazia Bruzzone [d], Domenico Aquino [d], Laura Biagi [e], Paolo Bosco [e], Irene Carne [f], Stefania Ferraro [d], Giovanni Giulietti [g,h], Antonio Napolitano [i], Anna Nigri [d], Luigi Pavone [j], Alice Pirastru [k], Alberto Redolfi [l], Fabrizio Tagliavini [m], Michela Tosetti [e], Marco Salvatore [a], Claudia A.M. Gandini Wheeler-Kingshott [n,c], Marco Aiello [a,*], the RIN – Neuroimaging Network[1]

[a] *IRCCS SYNLAB SDN, Naples, Italy*
[b] *IRCCS Humanitas Research Hospital, Rozzano, Italy*
[c] *Department of Brain and Behavioral Sciences, Università degli Studi di Pavia, Pavia, Italy*
[d] *Neuroradiology Unit, Fondazione IRCCS Istituto Neurologico Carlo Besta, Milan, Italy*
[e] *Laboratory of Medical Physics and Magnetic Resonance, IRCCS Stella Maris Foundation, Pisa, Italy*
[f] *Neuroradiology Unit, IRCCS Istituti Clinici Scientifici Maugeri, Pavia, Italy*
[g] *Neuroimaging Laboratory, IRCCS Santa Lucia Foundation, Rome, Italy*
[h] *SAIMLAL Department, Sapienza University of Rome, Rome, Italy*
[i] *Medical Physics, IRCCS Istituto Ospedale Pediatrico Bambino Gesù, Rome, Italy*
[j] *IRCCS Neuromed, Pozzilli, Italy*
[k] *IRCCS Fondazione Don Carlo Gnocchi Onlus, Milan, Italy*
[l] *Laboratory of Neuroinformatics, IRCCS Istituto Centro San Giovanni di Dio Fatebenefratelli, Brescia, Italy*
[m] *Scientific Direction, Fondazione IRCCS Istituto Neurologico Carlo Besta, Milan, Italy*
[n] *NMR Research Unit, Department of Neuroinflammation, Queen Square MS Centre, UCL Queen Square Institute of Neurology, Faculty of Brain Sciences, University College London, London, United Kingdom*

* Corresponding author at: IRCCS SYNLAB SDN Via Gianturco 113, 80143 Naples, Italy.
E-mail address: marco.aiello@synlab.it (M. Aiello).

[1] Egidio D'Angelo (Fondazione IRCSS Istituto Neurologico Naz.le Mondino, University of Pavia), Gianluigi Forloni (Istituto di Ricerche Farmacologiche Mario Negri IRCCS), Raffaele Agati (IRCCS Istituto delle Scienze Neurologiche di Bologna), Elisa Alberici (IRCCS Istituti Clinici Scientifici Maugeri), Carmelo Amato (Oasi Research Institute-IRCCS), Domenico Aquino (Fondazione IRCCS Istituto Neurologico Carlo Besta), Filippo Arrigoni (Istituto Scientifico, IRCCS E. Medea), Francesca Baglio (IRCCS Fondazione don Carlo Gnocchi onlus), Stefano Bastianello (Fondazione IRCSS Istituto Neurologico Naz.le Mondino), Lilla Bonanno (IRCCS Centro Neurolesi Bonino Pulejo), Francesca Bottino (IRCCS Istituto Ospedale Pediatrico Bambino Gesù), Marco Bozzali (Fondazione IRCCS Santa Lucia), Chiara Carducci (IRCCS Istituto Ospedale Pediatrico Bambino Gesù), Lorenzo Carnevale (IRCCS Neuromed), Antonella Castellano (IRCCS Ospedale San Raffaele), Mattia Colnaghi (Istituto Auxologico Italiano IRCCS), Giorgio Conte (Fondazione IRCCS Cà Granda Osp. Maggiore Policlinico), Mauro Costagli (University of Genova; Fondazione IRCCS Stella Maris), Silvia De Francesco (IRCCS Istituto Centro San Giovanni di Dio Fatebenefratelli), Greta Demichelis (Fondazione IRCCS Istituto Neurologico Carlo Besta), Valeria Elisa Contarino (Fondazione IRCCS Caâ Granda Osp. Maggiore Policlinico), Andrea Falini (IRCCS Ospedale San Raffaele), Giulio Ferrazzi (IRCCS Ospedale San Camillo), Lorenzo Figà Talamanca (IRCCS Istituto Ospedale Pediatrico Bambino Gesù), Cira Fundarò (IRCCS Istituti Clinici Scientifici Maugeri), Francesco Ghielmetti (Fondazione IRCCS Istituto Neurologico Carlo Besta), Ruben Gianeri (Fondazione IRCCS Istituto Neurologico Carlo Besta), Marco Grimaldi (IRCCS Istituto Clinico Humanitas), Antonella Iadanza (IRCCS Ospedale San Raffaele), Marta Lancione (Fondazione IRCCS Stella Maris), Fabrizio Levrero (IRCCS Ospedale Policlinico San Martino), Raffaele Lodi (IRCCS Istituto delle Scienze Neurologiche di Bologna), Daniela Longo (IRCCS Istituto Ospedale Pediatrico Bambino Gesù), Giulia Lucignani (IRCCS Istituto Ospedale Pediatrico Bambino Gesù), Martina Lucignani (IRCCS Istituto Ospedale Pediatrico Bambino Gesù), Maria Luisa Malosio (IRCCS Istituto Clinico Humanitas), Vittorio Manzo (Istituto Auxologico Italiano, IRCCS), M. Marcella Laganà (IRCCS Fondazione don Carlo Gnocchi onlus), Silvia Marino (IRCCS Centro Neurolesi Bonino Pulejo), Jean Paul Medina (Fondazione IRCCS Istituto Neurologico Carlo Besta), Edoardo Micotti (Istituto di Ricerche Farmacologiche Mario Negri IRCCS), Claudia Morelli (Istituto Auxologico Italiano IRCCS), Alessio Moscato (IRCCS Istituti Clinici Scientifici Maugeri), Francesco Padelli (Fondazione IRCCS Istituto Neurologico Carlo Besta), Patrizia Pantano (RCCS Neuromed), Chiara Parrillo (IRCCS Istituto Ospedale Pediatrico Bambino Gesù), Denis Peruzzo (Istituto Scientifico, IRCCS E. Medea), Nikolaos Petsas (IRCCS Neuromed), Letterio S. Politi (IRCCS Istituto Clinico Humanitas), Luca Roccatagliata (IRCCS Ospedale Policlinico San Martino), Elisa Rognone (Fondazione IRCSS Istituto Neurologico Naz.le Mondino), Andrea Rossi (Ospedale Pediatrico Istituto Giannina Gaslini, Università di Genova), Maria Camilla Rossi-Espagnet (IRCCS Istituto Ospedale Pediatrico Bambino Gesù), Claudia Ruvolo (IRCCS Centro Neurolesi Bonino Pulejo), Emanuela Tagliente (IRCCS Istituto Ospedale Pediatrico Bambino Gesù), Claudia Testa (IRCCS Istituto delle Scienze Neurologiche di Bologna), Caterina Tonon (IRCCS Istituto delle Scienze Neurologiche di Bologna), Domenico Tortora (Ospedale Pediatrico Istituto Giannina Gaslini), Fabio Maria Triulzi (Fondazione IRCCS Cà Granda Osp. Maggiore Policlinico).

https://doi.org/10.1016/j.ejmp.2023.102610
Received 30 October 2022; Received in revised form 20 March 2023; Accepted 30 May 2023
Available online 17 June 2023

ARTICLE INFO

Keywords:
Human connectome
Graph metrics
Reproducibility
Diffusion tractography

ABSTRACT

Purpose: The use of topological metrics to derive quantitative descriptors from structural connectomes is receiving increasing attention but deserves specific studies to investigate their reproducibility and variability in the clinical context. This work exploits the harmonization of diffusion-weighted acquisition for neuroimaging data performed by the Italian Neuroscience and Neurorehabilitation Network initiative to obtain normative values of topological metrics and to investigate their reproducibility and variability across centers.

Methods: Different topological metrics, at global and local level, were calculated on multishell diffusion-weighted data acquired at high-field (e.g. 3 T) Magnetic Resonance Imaging scanners in 13 different centers, following the harmonization of the acquisition protocol, on young and healthy adults. A "traveling brains" dataset acquired on a subgroup of subjects at 3 different centers was also analyzed as reference data. All data were processed following a common processing pipeline that includes data pre-processing, tractography, generation of structural connectomes and calculation of graph-based metrics.

The results were evaluated both with statistical analysis of variability and consistency among sites with the traveling brains range. In addition, inter-site reproducibility was assessed in terms of intra-class correlation variability.

Results: The results show an inter-center and inter-subject variability of <10%, except for "clustering coefficient" (variability of 30%). Statistical analysis identifies significant differences among sites, as expected given the wide range of scanners' hardware.

Conclusions: The results show low variability of connectivity topological metrics across sites running a harmonised protocol.

1. Introduction

Structural connectome analysis through graph metrics has demonstrated to be a powerful tool to study, in vivo, the brain organization. Indeed, the analysis of topological properties of the structural connectome has gained particular attention in clinical neurosciences due to its ability to reveal hidden brain alterations related to different brain disorders [1,2] or brain injuries [3]. However, the entire process to derive structural connectomes and graph metrics may be strongly influenced by different factors related to acquisition strategies, coil systems, scanners, and pipelines for tractography reconstruction and connectome generation [4–6]. In this context, efforts have been made to standardize acquisition protocols and processing pipelines for data harmonization purposes [7–11]. However, the reliability of graph-based connectome analysis, as revealed by diffusion tractography, has been under-investigated in terms of across sites normative values. To this end, in recent years, national and international multicentre initiatives for the standardization and harmonization of protocols have been pursued, which are releasing valuable datasets to be suitably analyzed [12–14].

The Neuroscience and Neurorehabilitation Network (RIN), the Italian largest research network in the neuroscience field, was funded in 2017 by the Italian Ministry of Health. The RIN drives the collaboration among several Scientific Institutes of Hospitalization and Care (IRCCSs), i.e. Italian Research Hospitals, to pursue the shared goal of identifying disease and subject-specific in-vivo neuroimaging biomarkers for different neurological and neuropsychiatric conditions [15]. The main activities of the RIN, during its early phases, were essentially: i) definition of protocols and procedures for the harmonization of high-field MRI scanners in centres belonging to the network; ii) acquisition of a normative population sample to study multi-centric reproducibility of harmonized protocols; iii) apply the harmonized protocol to clinical research. As a result, these activities returned a fundamental data resource for probing the reliability of advanced MR examinations and processing pipelines [16,17]. The aim of this work consists precisely in exploiting the normative data of the RIN network to demonstrate the degree of multi-centric reproducibility of topological descriptors of the healthy connectome and, therefore, to evaluate their use as normative values of a young population.

To the best of our knowledge, there are no studies investigating multicenter reproducibility of human connectome's graph metrics on harmonized protocols. In fact, although the issue of reliability of topological metrics has been extensively addressed in numerous studies in terms of test–retest reproducibility [18–24], multicentric reproducibility is still under investigated.

2. Material and Methods

2.1. Subjects' characteristics

As part of the optimization protocol, a technical team of RIN members was in charge of setting up a shared acquisition protocol, which included a multi-shell diffusion sequence. In order to assess the across-sites reproducibility, a "traveling brains" test was performed. In details, four volunteers, balanced for gender and with an age range of 30–35 years, were scanned at three representative sites (i.e. 1, 4 and 6 of Table 1) following the finalized protocol detailed in Table 2.

Once the acquisition protocol was agreed [15], it was installed at each centre and a dummy scan acquired to confirm that the standard

Table 1
Demographic and MR scanner details of the multi-centric study.

Site	1	2	3	4	5	6	7	8	9	10	11	12	13
Age (#)	31.8 ± 1.8 (3)	29.6 ± 2.7 (5)	29.7 ± 4.3 (6)	26.3 ± 5.9 (6)	28.0 ± 2.3 (5)	30.0 ± 4.4 (5)	32.2 ± 3.0 (5)	31.8 ± 5.2 (5)	25.0 ± 2.0 (3)	31.6 ± 6.3 (5)	25.1 ± 3.3 (7)	29.2 ± 3.0 (5)	28.5 ± 5.6 (4)
Gender (F/M)	1/2	4/1	5/1	4/2	1/4	3/2	3/2	3/2	1/2	4/1	6/1	2/3	2/2
MRI vendor	V1	V2	V1	V3	V3	V2	V3	V1	V1	V1	V3	V3	V2
RF head-coil	SENSE-Head-32	SENSE-Head-32	SENSE-Head-32	Head-Neck 64	HeadMatrix-4	HNS (8ch)	SENSE-Head-32	SENSE-Head-32	SENSE-Head-32	SENSE-Head-32	Head-Neck 64	Head-Neck 16	Head-Neck 32

Table 2
Details of the harmonized imaging protocols for both structural and diffusion-weighted imaging acquisitions.

Parameters	T1-weighted			DWI		
Vendors	Philips	Siemens	GE	Philips	Siemens	GE
Sequence type	3D FFE	MP-RAGE	3D BRAVO	Single shot SE EPI	EPI SE 2D	2D SE EPI
Slice orientation	sagittal	sagittal	sagittal	transversal	transversal	oblique
FOV [mm]	240 × 240	256 × 256	256 × 256	240 × 240	240 × 240	240 × 240
Resolution [mm^3]	1 × 1 × 1	1 × 1 × 1	1 × 1 × 1	2.5 × 2.5 × 2.5	2.5 × 2.5 × 2.5	2.5 × 2.5 × 2.5
Matrix (Base Resolution)	240 × 240	256 × 256	256 × 256	96 × 96	96 × 96	96 × 96
Slice thickness	1	1	1	2.5	2.5	2.5
n. slices	175–180	175–180	175–180	60	60	60
Phase Encoding direction	AP	AP	PA (non modif)	PA	PA	PA
Slice order	Interleaved	Interleaved	Interleaved	interleaved	interleaved	interleaved
TR [ms]	shortest	2300	non modif	8400	8400	8400
TE [ms]	shortest	2.96	3.2	85	85	85
Flip angle	8°	9°	9°	90°	90°	90°
Fat suppression	No	No	No	yes	yes	yes
Acceleration factor	SENSE ≤ 2.3	GRAPPA = 2	ARC = 2	SENSE ≤ 2.3	GRAPPA = 2	ASSET = 2
n. directions/ b0	–	–	–	32 dir / 7 b0	30 dir / 7 b0	32 dir / 4 b0
b [s/mm^2]	–	–	–	1000/2000	1000/2000	1000/2000
Bandwidth	191 Hz	240 Hz/Px	31.25 kHz	1040 Hz	1108 Hz/px	250 kHz
Duration [min]	≈**5.30**			≈**10**		

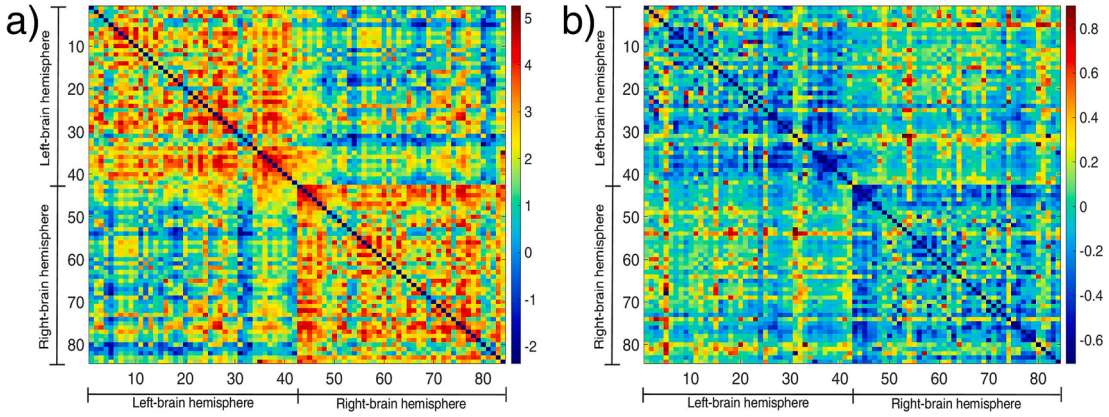

Fig. 1. Across-subjects mean (a) and coefficient of variation (b) of structural connectomes (fiber count) of the RIN dataset (64 subjects). A base-10 logarithmic scale has been used to enhance visualizations. Please refer to Table S1 for the association between node index and gray matter region.

Table 3
Normative values and coefficients of variation estimated across all "traveling brains" subjects and sites (1,4,6) for the global graph metrics. The last column shows ICC coefficients. Median and IQR values correspond to the average median and IQR between each subject in the "traveling brains" experiment. mCoV = mean coefficient of variation; IQR = interquartile range; ICC = intraclass correlation coefficient.

	Median	IQR	mCoV	ICC
Betweenness Centrality	55.49	2.23	0.03	0.15
Clustering Coefficient	7.93×10^{-3}	2.49×10^{-3}	0.22	0.74
Degree	5.78×10^{4}	4.34×10^{3}	0.05	0.89
Global Efficiency	2.71×10^{3}	215.67	0.06	0.71
Local Efficiency	4.23×10^{3}	306.26	0.05	0.62
Path Length	7.49×10^{-5}	6.25×10^{-6}	0.06	0.70

operating procedures were clear and followed by all. Each center of the RIN network was required to acquire at least three cognitively and neurologically healthy subjects aged between 20 and 40 years. Each subject underwent a neurocognitive evaluation and the MRI harmonized protocol [15], summarized below for simplicity.

For each site of the RIN network, Table 1. shows the details of both the subjects included in the study and the MR hardware available for the acquisition.

A total of 64 healthy subjects (age range: 21–38 years, mean ± standard deviation: 29.1 ± 4.5 years, median: 29 years, 24 women) were enrolled from 2018 to 2020.

Table 4
Normative values reported as median and interquartile range (IQR) and coefficients of variation (CoV) estimated across all subjects and sites for the global graph metrics.

	Median	IQR	CoV
Betweenness centrality	55.30	6.40	0.08
Clustering Coefficient	8.09×10^{-3}	4.00×10^{-3}	0.31
Degree	5.84×10^{4}	3.69×10^{3}	0.05
Global Efficiency	2.72×10^{3}	213.04	0.06
Local Efficiency	4.29×10^{3}	363.59	0.07
Path Length	7.44×10^{-5}	5.94×10^{-6}	0.07

2.2. MRI acquisition

Table 2 shows the details of the harmonized structural and diffusion-weighted imaging protocols setup per MR vendor.

T1 sequences follow a protocol with isotropic resolution of 1 mm^3 and parallel imaging acceleration factor of 2. Regarding the diffusion-weighted imaging sequences, the protocol consists of the acquisition of 30 diffusion directions with two diffusion weightings (1000 s / mm^2 and 2000 s / mm^2), 7 volumes with zero b-value and an isotropic resolution of 2.5x2.5x2.5 mm^3. An additional diffusion-weighted imaging

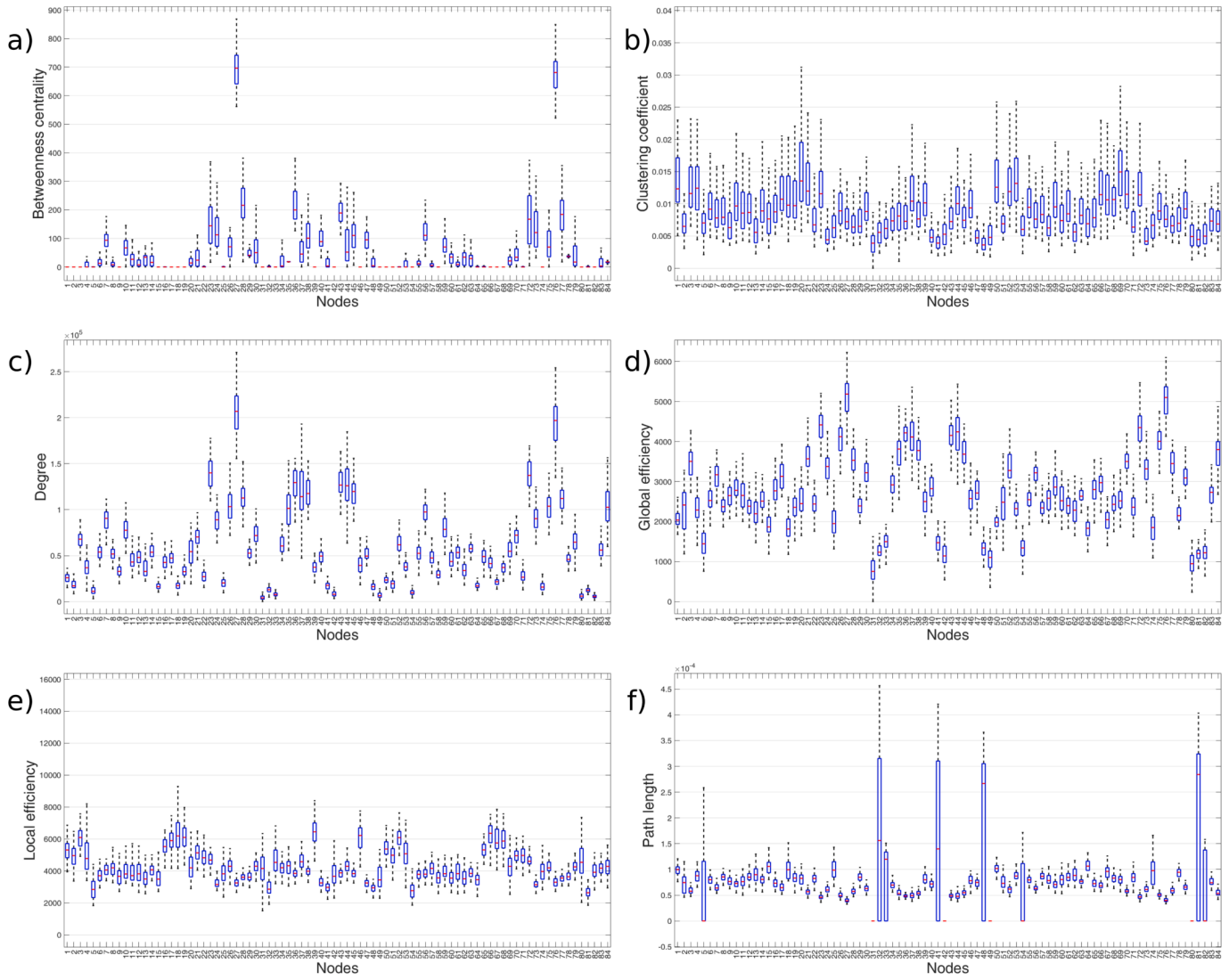

Fig. 2. Boxplots of local graph metric distributions. Each panel shows the data distribution across the subjects of a specific local graph metric (betweenness centrality (a), clustering coefficient (b), degree (c), global efficiency (d), local efficiency (e) and path length (f)). For each boxplot, the x-axis represents node indices. Please refer to Table S1 for the association between node index and related gray matter region.

set of 3 volumes with zero b-value was acquired with the same parameters only by reversing the phase-encoding direction (i.e. anterior-posterior), suitable for the following geometric distortion correction routine.

2.3. Data processing

For the following processing steps, a combination of commands from MRtrix3 (version 3.0.3, [25]) and FMRIB-FSL (version 6.0, [26]) toolboxes were adopted [27].

Diffusion data were firstly pre-processed to mitigate potential image artifacts. In particular, the images were denoised by applying the Machenko-Pastur PCA noise removal technique [28] and corrected for gibbs-ringing artifacts [29] using *mrdegibbs* command of MRtrix3 toolbox. Then, distortion correction was performed by using the data with 0 s / mm^2 diffusion weighting, acquired with reversed phase-encoding direction (anterior-posterior) by means of susceptibility-induced off-resonance field estimation [30]. Moreover, eddy current-induced distortions and artifacts due to subject movement were mitigated by running *eddy* from the FSL software library, which is an integrated method of correction, as described in [31]. Finally, diffusion-weighted data were corrected for B1 field inhomogeneity [32] applying *dwibiascorrect* routine of MRtrix3 toolbox.

From the diffusion-weighted pre-processed images, fractional anisotropy (FA) parametric map was evaluated from the eigenvalues of the diffusion tensor by MRTrix3 toolbox and axonal streamlines were reconstructed by applying a probabilistic tractography approach based on multi-shell multi-tissue constrained spherical deconvolution [33]. For the streamline reconstruction procedure, T1-weighted image was registered to diffusion-weighted image space by affine transform with 12 degree of freedom and "trilinear" interpolation method by means of flirt routine of FSL toolbox. Tissue segmentation (i.e. white matter, gray matter and cerebrospinal fluid) for the multi-tissue approach was obtained with 5ttgen command of MRtrix3 that includes bet, fast and first routines of FSL software library for brain extraction, tissue and subcortical gray matter segmentation, respectively. The parameters for tractography reconstructions were as follows: [2.5–250] mm as range of included streamline length, 10^7 as number of selected streamlines, 60° as angle constraint. In the tractography reconstruction procedure, the anatomically-constrained method [34] was used to apply biologically realistic constraints for streamline termination.

Gray matter parcellation was obtained by applying the cross-sectional RECON-ALL routine from the Freesurfer package (version 7.2, [35]) to the T1-weighted images in native space. Following the

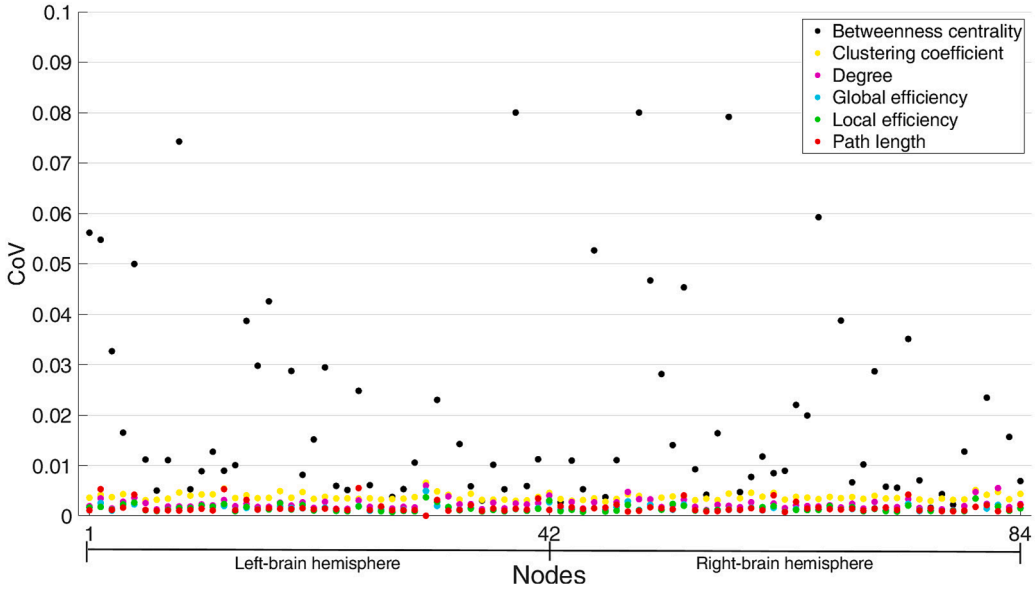

Fig. 3. Across-subjects coefficient of variation. The plot shows the coefficient of variation (CoV) of the graph metrics for each node (x-axis) estimated across-subjects. Please refer to Table S1 for the association between node index and gray matter region. Different colours of the plotted points are associated with different graph metrics.

Desikan-Killiany atlas [36], 84 cortical and subcortical gray matter regions of interest (ROIs) were extracted (Table S2).

To obtain structural connectomes, the number of reconstructed streamlines connecting each pair of ROIs was evaluated, thus resulting in 84x84 symmetric matrices of structural connectivity. In addition to streamline count, structural connectomes with edges weighted by FA (FA-conn) and scaled by the inverse of corresponding node volumes (VOL-conn) were evaluated. The structural connectomes were filtered by the spherical-deconvolution informed filtering of the tractogram approach, as described in [37], to produce more biologically plausible measurements with respect to fiber orientation distributions.

Graph analysis was performed with the open-source GRETNA toolbox [38].

The following graph metrics, both at global network and node level, were calculated on each structural connectome: betweenness centrality (BC), clustering coefficient (CC), degree (D), global efficiency (GL), local efficiency (LE) and path length (PL). BC represents the fraction of all shortest path, CC is the fraction of node's neighbors that are neighbors of each other, D is the number of the links connecting the nodes, GE and LE represent the average inverse shortest path length in the network and with respect to the neighborhood of the node respectively, and PL is average shortest path length. As already described in [19], the resulting graph metrics were normalized by graph metrics derived with 100 random networks with the same node, edge and degree distribution by means of Maslov-Sneppen rewiring algorithm [39].

2.4. Statistical analysis

Regarding the "traveling brains" test, across sites reproducibility was evaluated by means of both within-subject coefficient of variation (CoV) and intra-class coefficient (ICC) [40]. In particular, the two-ways random effects model with absolute agreement ICC was evaluated as:

$$ICC = \frac{MS_b - MS_W}{MS_b + (k-1)MS_w}$$

where MS_b and MS_W respectively represent between- and within-subject mean squares and k is the number of repeated measurements. CoV values < 0.1 represent low variability between the measurements [41], while ICC values above 0.7 reflect highly reproducible measurements [41].

Across-site differences in demographic variables as gender and age were analysed by one-way Kruskal-Wallis test.

To provide normative values of the analyzed dataset, median and interquartile range were evaluated for each graph metric. Moreover, the between-subjects CoV was calculated, for each graph metric, as the ratio between the standard deviation and the mean value of the entire dataset [42].

Kruskal-Wallis test was applied to assess the influence of different sites on graph metrics with Fisher's least significant difference as a post-hoc test for pairwise comparisons and honestly significant difference test was adopted as correction technique for multiple comparison. $P < 0.05$ was considered as significant threshold for all the performed statistical tests.

All the statistical analyses were performed using MATLAB r2018a (Mathworks, Inc.).

3. Results

In Fig. 1 and figure S1 the mean structural connectomes of the entire RIN dataset was shown, whereas in table S2 the graph metrics values for each subject of the "traveling brains" experiment were reported.

Regarding subjects' age, no significant differences across sites were found ($p = 0.59$). On the contrary, the inter-site gender distribution significantly differed across sites ($p < 0.05$).

Considering the "traveling brains" experiment, the results shown in Table 3. were appreciably reproducible on the three sites both in terms of CoV (always lower than 0.1) and ICC, with the exception of BC metric (ICC = 0.15). This is confirmed also when the analysis was performed by considering FA-conn and VOL-conn (table S3).

Table 4 and Fig. 2 show the normative results for the global and local metrics, respectively. Moreover, the corresponding global and local metric values arising from FA-conn and VOL-conn were reported in table S4 and figure S2. The coefficients of variation, reported in the last column of Table 4, showed a good degree of consistency and uniformity across all metrics, considering values under the threshold of 0.1, except for the CC metric both for connectomes weighted by streamline count and FA-conn (0.31 and 0.20, respectively). On the contrary, CoV values of CC, D, GE and LE evaluated from VOL-conn were between 0.15 and 0.30. The CoV of all local-level metrics was always acceptable, as shown

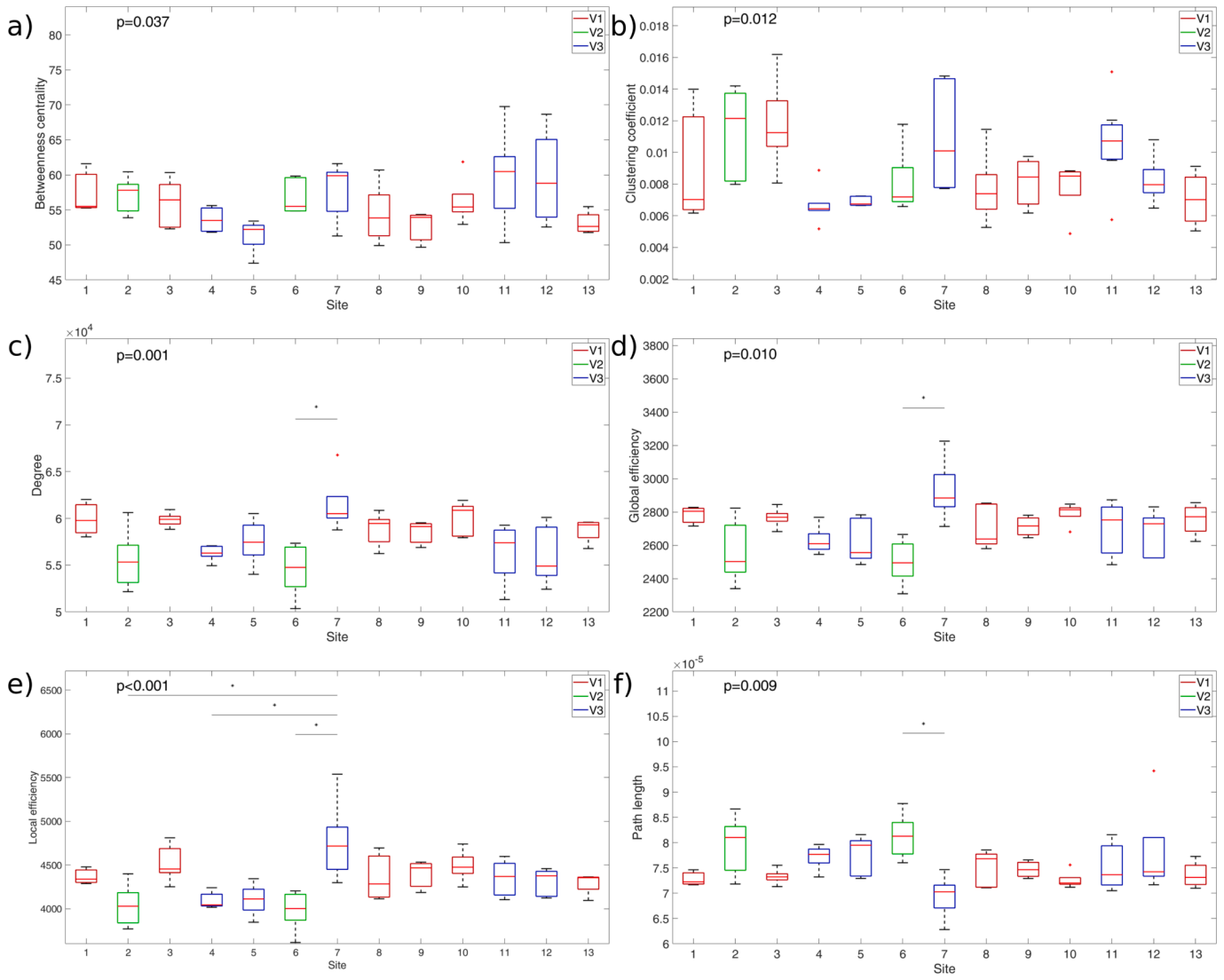

Fig. 4. Boxplots of graph metric distributions. The reported p-values are related to Kruskal-Wallis test to assess the influence of the sites on graph metrics. Each panel shows, for each site, the data distribution across the subjects of a specific global graph metric (betweenness centrality (a), clustering coefficient (b), degree (c), global efficiency (d), local efficiency (e) and path length (f)). Lines with asterisks indicate statistically significant differences (post-hoc test). Different colors of the boxplots are associated to different MR vendors (red: V1; green: V2; blue: V3). (For interpretation of the references to colour in this figure legend, the reader is referred to the web version of this article.)

in Fig. 3 and figure S4, as the CoVs of these metrics for each graph node were all below 0.1.

Fig. 4 and figures S5-S6 show the boxplots of graph metrics distributions across subjects, reported for each site. The Kruskal-Wallis test showed a statistically significant influence of the variable "sites" on the distribution of the metrics only when streamline count was adopted for connectome weighting (Fig. 4); it is important to note, however, that as visually evident and as confirmed by Fisher's post-hoc test, the results from site 6 have a noticeable impact on these differences.

4. Discussion

In this paper, we demonstrated the value of a harmonized diffusion weighted imaging protocol, adopted for a national multicenter study [15], in defining the healthy brain connectome and its normative topological values. In particular, the present study focused on the computation of topological parameters extracted from structural connectomes based on diffusion MR sequences acquired on 13 different high-field scanners.

Overall, the results show good consistency and homogeneity of the distribution of normative values in a population of young adults, considering all the acquisition sites.

Specifically, of 6 metrics examined in this study, only the global CC shows CoV higher than 0.1, with CoV of 0.31. This variability was also partially confirmed in the "traveling brains" experiment (mCoV of 0.22 and 0.18 for connectomes weighted by streamline count and VOL-conn, respectively).

Similarly, the BC metric also shows the worst test–retest reproducibility value for all the analyzed connectome weightings. These results are in line with what is already evident in the literature: in [19], using the same processing pipeline as us (iFOD2 with a multishell diffusion-weighted acquisition scheme), BC metric results in worst reproducibility performance while [23] showed excellent single site reproducibility of graph metrics with the exception of the BC itself. It is important to underline that BC considers nodes along the shortest geodesic paths to be the most central in the network; although it is widely used as a topological measure of brain organization, it is not ideal for a system that processes information via unrestricted walks such as the human brain [43]. Brain dynamics, indeed, imply a certain independency of information flow efficiency from the shortest paths, which may be an

explanation of the variability found in the BC metric.

Regarding the CC metric, the huge variability found in the normative values of our multicentre study does not seem to be affected by appreciable differences at the level of sites. Hence, the variability of the CC metric is more sensitive to subjective variations than to instrumental differences. Moreover, it should be considered that the CC metric, as confirmed by our traveling brains results, is highly reproducible when reconstruction techniques that produce poorly sparse connectomes are considered, as in the case of this work. In fact, CC, which estimates the degree to which nodes in a graph tend to cluster together, is highly robust with respect to a possible path loss between test and retest [44].

This study is subject to some considerations. First, as shown by the statistical analysis of independence, there is no gender balance among data from different centers; considering that gender is reported to be affecting graph-based metrics for intrinsic differences in inter-hemispheric communication between males and females [45], such differences should be taken into account in the interpretation of our across-sites results. Furthermore, we should also consider that some of the centers acquired a different number of subjects, which in turn may have influenced the site results. It is worth mentioning, also that, due to the limited number of subjects per site, the influence of different technical setup (e.g. MR scanner model, software version and RF head-coil) among sites was not considered, hence requiring further studies to assess their impact on the variability of normative graph metric values. It is important to note that dedicated post-acquisition procedures can be used to mitigate the inter-scanner variability in case of harmonised acquisition protocols, as recently proved as a solution to possibly improve reproducibility [9].

In the present work the choice of brain network metrics, related to network integration and segregation properties [46], was motivated since they were demonstrated to be relevant for studies focused on neurodegenerative and neurodevelopmental diseases [1]. However, the description of structural brain connectivity properties by means of path- and cluster-based graph metrics should be used with caution due to the potentially missing relationship between network topology measurements and the underlying neurobiology [47].

In conclusion, the study of the variability of the topological parameters calculated from data acquired at different sites is fundamental to assess reliability and to favor the use of these descriptors as markers of a pathological, neuropsychological or behavioral condition. With this study, normative values of topological metrics were shared by providing an indication of the “real-world” variability, considering 13 different acquisition sites with different MR scanners produced by three different vendors and with different setups. The results, overall, show acceptable reproducibility of graph metrics across centres who are running a harmonised protocol, with CoVs mostly within 10%. Graph theory metrics could therefore be used in multicentre clinical trials as imaging biomarkers of brain connectivity.

Funding

This project was funded by the Italian Minister of Health (RCR; RRC-2016-2361095; RRC-2017-2364915; RRC-2018-2365796; RCR-2019-23669119_001; RCR-2022-23682285; GR-2018-12366779) and the Ministry of Economy and Finance (CCR-2017-23669078). This study was also partially funded by “Ricerca Corrente” grant of Italian MoH and the 5x1000 voluntary contributions to IRCCS SYNLAB SDN. The funding sources had no role in the design and conduct of the study; in the collection, analysis, and interpretation of the data; or in the preparation, review, and approval of the manuscript.

Declaration of Competing Interest

The authors declare that they have no known competing financial interests or personal relationships that could have appeared to influence the work reported in this paper.

Appendix A. Supplementary data

Supplementary data to this article can be found online at https://doi.org/10.1016/j.ejmp.2023.102610.

References

[1] Griffa A, Baumann PS, Thiran J-P, Hagmann P. Structural connectomics in brain diseases. Neuroimage 2013;80:515–26. https://doi.org/10.1016/j.neuroimage.2013.04.056.
[2] Liu J, Li M, Pan Yi, Lan W, Zheng R, Wu F-X, et al. Complex Brain Network Analysis and Its Applications to Brain Disorders: A Survey. Complexity 2017;2017:1–27.
[3] Imms P, Clemente A, Cook M, D'Souza W, Wilson PH, Jones DK, et al. The structural connectome in traumatic brain injury: A meta-analysis of graph metrics. Neurosci Biobehav Rev 2019;99:128–37.
[4] Nath V, Schilling KG, Parvathaneni P, Huo Y, Blaber JA, Hainline AE, et al. Tractography reproducibility challenge with empirical data (TraCED): The 2017 ISMRM diffusion study group challenge. J Magn Reson Imaging 2020;51(1):234–49.
[5] Ning L, Bonet-Carne E, Grussu F, Sepehrband F, Kaden E, Veraart J, et al. Cross-scanner and cross-protocol multi-shell diffusion MRI data harmonization: Algorithms and results. Neuroimage 2020;221:117128.
[6] Schilling KG, Rheault F, Petit L, Hansen CB, Nath V, Yeh F-C, et al. Tractography dissection variability: What happens when 42 groups dissect 14 white matter bundles on the same dataset? Neuroimage 2021;243:118502. https://doi.org/10.1016/j.neuroimage.2021.118502.
[7] Cetin Karayumak S, Bouix S, Ning L, James A, Crow T, Shenton M, et al. Retrospective harmonization of multi-site diffusion MRI data acquired with different acquisition parameters. Neuroimage 2019;184:180–200.
[8] Fortin J-P, Parker D, Tunç B, Watanabe T, Elliott MA, Ruparel K, et al. Harmonization of multi-site diffusion tensor imaging data. Neuroimage 2017;161:149–70.
[9] Mirzaalian H, Ning L, Savadjiev P, Pasternak O, Bouix S, Michailovich O, et al. Multi-site harmonization of diffusion MRI data in a registration framework. Brain Imaging Behav 2018;12(1):284–95.
[10] Monti S, Pontillo G, Russo C, Cella L, Cocozza S, Palma G. RESUME : A flexible class of multi-parameter qMRI protocols. Phys Med 2021;88:23–36. https://doi.org/10.1016/j.ejmp.2021.04.005.
[11] Monti S, Borrelli P, Tedeschi E, Cocozza S, Palma G, Jiang Q. RESUME: Turning an SWI acquisition into a fast qMRI protocol. PLoS One 2017;12(12):e0189933.
[12] Jovicich J, Minati L, Marizzoni M, Marchitelli R, Sala-Llonch R, Bartrés-Faz D, et al. Longitudinal reproducibility of default-mode network connectivity in healthy elderly participants: A multicentric resting-state fMRI study. Neuroimage 2016;124:442–54.
[13] Jovicich J, Marizzoni M, Bosch B, Bartrés-Faz D, Arnold J, Benninghoff J, et al. Multisite longitudinal reliability of tract-based spatial statistics in diffusion tensor imaging of healthy elderly subjects. Neuroimage 2014;101:390–403.
[14] Marchitelli R, Minati L, Marizzoni M, Bosch B, Bartrés-Faz D, Müller BW, et al. Test-retest reliability of the default mode network in a multi-centric fMRI study of healthy elderly: Effects of data-driven physiological noise correction techniques. Hum Brain Mapp 2016;37(6):2114–32.
[15] Nigri A, Ferraro S, Gandini Wheeler-Kingshott CAM, Tosetti M, Redolfi A, Forloni G, et al. Quantitative MRI Harmonization to Maximize Clinical Impact: The RIN–Neuroimaging Network. Front Neurol 2022;13:855125. https://doi.org/10.3389/fneur.2022.855125.
[16] Palesi F, Nigri A, Gianeri R, Aquino D, Redolfi A, Biagi L, et al. MRI data quality assessment for the RIN - Neuroimaging Network using the ACR phantoms. Phys Med 2022;104:93–100.
[17] Lancione M, Bosco P, Costagli M, Nigri A, Aquino D, Carne I, et al. Multi-centre and multi-vendor reproducibility of a standardized protocol for quantitative susceptibility Mapping of the human brain at 3T. Phys Med 2022;103:37–45.
[18] Bonilha L, Gleichgerrcht E, Fridriksson J, Rorden C, Breedlove JL, Nesland T, et al. Reproducibility of the Structural Brain Connectome Derived from Diffusion Tensor Imaging. PLoS One 2015;10(9):e0135247.
[19] Borrelli P, Cavaliere C, Salvatore M, Jovicich J, Aiello M. Structural Brain Network Reproducibility: Influence of Different Diffusion Acquisition and Tractography Reconstruction Schemes on Graph Metrics. Brain Connect 2022;12:754–67. https://doi.org/10.1089/brain.2021.0123.
[20] Duda JT, Cook PA, Gee JC. Reproducibility of graph metrics of human brain structural networks. Front Neuroinform 2014:8. https://doi.org/10.3389/fninf.2014.00046.
[21] Messaritaki E, Dimitriadis SI, Jones DK. Optimization of graph construction can significantly increase the power of structural brain network studies. Neuroimage 2019;199:495–511. https://doi.org/10.1016/j.neuroimage.2019.05.052.
[22] Prčkovska V, Rodrigues P, Puigdellivol Sanchez A, Ramos M, Andorra M, Martinez-Heras E, et al. Reproducibility of the Structural Connectome Reconstruction across Diffusion Methods. J Neuroimaging 2016;26(1):46–57.
[23] Roine T, Jeurissen B, Perrone D, Aelterman J, Philips W, Sijbers J, et al. Reproducibility and intercorrelation of graph theoretical measures in structural brain connectivity networks. Med Image Anal 2019;52:56–67.
[24] Tsai S-Y. Reproducibility of structural brain connectivity and network metrics using probabilistic diffusion tractography. Sci Rep 2018;8:1–12. https://doi.org/10.1038/s41598-018-29943-0.

[25] Tournier J-D, Smith R, Raffelt D, Tabbara R, Dhollander T, Pietsch M, et al. MRtrix3: A fast, flexible and open software framework for medical image processing and visualisation. Neuroimage 2019;202:116137.
[26] Jenkinson M, Beckmann CF, Behrens TEJ, Woolrich MW, Smith SM. FSL. FSL NeuroImage 2012;62(2):782–90.
[27] Ades-Aron B, Veraart J, Kochunov P, McGuire S, Sherman P, Kellner E, et al. Evaluation of the accuracy and precision of the diffusion parameter EStImation with Gibbs and NoisE removal pipeline. Neuroimage 2018;183:532–43.
[28] Veraart J, Novikov DS, Christiaens D, Ades-aron B, Sijbers J, Fieremans E. Denoising of diffusion MRI using random matrix theory. Neuroimage 2016;142:394–406. https://doi.org/10.1016/j.neuroimage.2016.08.016.
[29] Kellner E, Dhital B, Kiselev VG, Reisert M. Gibbs-ringing artifact removal based on local subvoxel-shifts. Magn Reson Med 2016;76:1574–81. https://doi.org/10.1002/mrm.26054.
[30] Andersson JLR, Skare S, Ashburner J. How to correct susceptibility distortions in spin-echo echo-planar images: application to diffusion tensor imaging. Neuroimage 2003;20:870–88. https://doi.org/10.1016/S1053-8119(03)00336-7.
[31] Andersson JLR, Sotiropoulos SN. An integrated approach to correction for off-resonance effects and subject movement in diffusion MR imaging. Neuroimage 2016;125:1063–78. https://doi.org/10.1016/j.neuroimage.2015.10.019.
[32] Tustison NJ, Avants BB, Cook PA, Yuanjie Zheng, Egan A, Yushkevich PA, et al. N4ITK: improved N3 bias correction. IEEE Trans Med Imaging 2010;29(6):1310–20.
[33] Jeurissen B, Tournier J-D, Dhollander T, Connelly A, Sijbers J. Multi-tissue constrained spherical deconvolution for improved analysis of multi-shell diffusion MRI data. Neuroimage 2014;103:411–26. https://doi.org/10.1016/j.neuroimage.2014.07.061.
[34] Smith RE, Tournier J-D, Calamante F, Connelly A. Anatomically-constrained tractography: Improved diffusion MRI streamlines tractography through effective use of anatomical information. Neuroimage 2012;62:1924–38. https://doi.org/10.1016/j.neuroimage.2012.06.005.
[35] Dale AM, Fischl B, Sereno MI. Cortical Surface-Based Analysis: I. Segmentation and Surface Reconstruction. NeuroImage 1999;9:179–94. https://doi.org/10.1006/nimg.1998.0395.
[36] Desikan RS, Ségonne F, Fischl B, Quinn BT, Dickerson BC, Blacker D, et al. An automated labeling system for subdividing the human cerebral cortex on MRI scans into gyral based regions of interest. Neuroimage 2006;31(3):968–80.
[37] Smith RE, Tournier J-D, Calamante F, Connelly A. SIFT2: Enabling dense quantitative assessment of brain white matter connectivity using streamlines tractography. Neuroimage 2015;119:338–51. https://doi.org/10.1016/j.neuroimage.2015.06.092.
[38] Wang J, Wang X, Xia M, Liao X, Evans A, He Y. GRETNA: a graph theoretical network analysis toolbox for imaging connectomics. Front Hum Neurosci 2015:9. https://doi.org/10.3389/fnhum.2015.00386.
[39] Maslov S, Sneppen K. Specificity and Stability in Topology of Protein Networks. Science 2002;296:910–3. https://doi.org/10.1126/science.1065103.
[40] McGraw KO, Wong SP. Forming inferences about some intraclass correlation coefficients. Psychol Methods 1996;1:30–46. https://doi.org/10.1037/1082-989X.1.1.30.
[41] Marenco S, Rawlings R, Rohde GK, Barnett AS, Honea RA, Pierpaoli C, et al. Regional distribution of measurement error in diffusion tensor imaging. Psychiatry Res 2006;147(1):69–78.
[42] Bland JM, Altman DG. Statistics Notes: Measurement error proportional to the mean. BMJ 1996;313. https://doi.org/10.1136/bmj.313.7049.106.
[43] Joyce KE, Laurienti PJ, Burdette JH, Hayasaka S, Sporns O. A New Measure of Centrality for Brain Networks. PLoS One 2010;5(8):e12200.
[44] Dennis EL, Jahanshad N, Toga AW, McMahon KL, de Zubicaray GI, Martin NG, et al. Test-Retest Reliability of Graph Theory Measures of Structural Brain Connectivity. In: Ayache N, Delingette H, Golland P, Mori K, editors. Medical Image Computing and Computer-Assisted Intervention – MICCAI 2012, vol. 7512, Berlin, Heidelberg: Springer Berlin Heidelberg; 2012, p. 305–12. 10.1007/978-3-642-33454-2_38.
[45] Tyan Y-S, Liao J-R, Shen C-Y, Lin Y-C, Weng J-C. Gender differences in the structural connectome of the teenage brain revealed by generalized q-sampling MRI. NeuroImage: Clinical 2017;15:376–82. https://doi.org/10.1016/j.nicl.2017.05.014.
[46] Sporns O. Graph theory methods: applications in brain networks. Transl Res 2018;20:11.
[47] Fornito A, Zalesky A, Breakspear M. Graph analysis of the human connectome: Promise, progress, and pitfalls. Neuroimage 2013;80:426–44. https://doi.org/10.1016/j.neuroimage.2013.04.087.